

Asymmetric quantum transport in a double-stranded Kronig-Penney model

Taksu Cheon, Sergey S. Poghosyan

Laboratory of Physics, Kochi University of Technology, Tosa Yamada, Kochi 782-8502, Japan

Abstract

We introduce a double-stranded Kronig-Penney model and analyze its transport properties. The asymmetric fluxes between two strands with suddenly alternating localization patterns are found as the energy is varied. The zero-size limit of the internal lines connecting two strands is examined using quantum graph vertices with four edges. We also consider a two-dimensional Kronig-Penney lattice with two types of alternating layers with δ and δ' connections, and show that the existence of energy bands in which the quantum flux can flow only in selected directions.

Keywords: solvable quantum mechanics, periodic potential, exotic vertex

PACS: 03.65.-w, 03.65.Nk, 73.63.Nm

1. Introduction

The investigation of wave propagation through periodic networks [1, 2] has been motivated by problems of free-electron motion on organic molecules and quantum wires. The application of more complicated graph structures was found also in other areas such as quantum chaos, photonic crystals, dynamical systems and nanotechnologies [3]. Mathematically, quantum graphs arise when one considers a propagation of waves through quasi-one-dimensional systems in the limit cases. The study of periodic quantum graphs with *non-conventional graph vertices* [4] has brought a new vista to the problem by revealing exotic particle dynamics, which were not found in models with the commonly used δ -potential type vertices. [5, 6, 7]

In this paper, we follow that lead and consider double-stranded periodic quantum graphs in the form of chained rings, with non-conventional four-way junction nodes. The model can be regarded as the two-lane extension of celebrated Kronig-Penney model, [8] which is a prototype of solvable system possessing of the band spectra. We show that, with the proper tuning of parameters, this system exhibits the energy bands in which quantum fluxes show the asymmetry between two strands, both in terms of relative strengths and direction. Moreover, the mode of asymmetry goes through a sudden change when the particle energy is varied and the system moves from one band to another. The pattern of change of the flux asymmetry is shown to be quite various depending on the choice of system parameters.

Email addresses: taksu.cheon@kochi-tech.ac.jp (Taksu Cheon), sergey.poghosyan@kochi-tech.ac.jp (Sergey S. Poghosyan)

In order to check that the flux asymmetry is not a particular feature of the specific model of chained rings, we also consider a ladder type double-stranded model with two straight strands connected by periodic internal lines. For this model we employ a three-way graph vertex of δ and δ' type couplings. We confirm that the flux asymmetry that varies from one band to the other is observed in this type of model as well.

It is essential that we are able to approximate Kronig-Penney lattices with non-conventional junctions, in terms of physically realizable vertex couplings. As is well known, the δ -potential vertex can be realised as the short-range limit of any regular potential with scaled potential strength that keeps its volume integral constant. It has been recently found that the vertices with the most general singular couplings can be approximated by auxiliary graphs, carrying only δ potentials and a magnetic field [9]. We explicitly construct finite ladders with only δ couplings, thus presenting the experimentally constructible double-stranded periodic quantum graph with two outer strands and many internal lines.

The paper is organised as follows: In section 2, a double-stranded Kronig-Penney model in the form of chained rings is presented, and its characteristics of flux asymmetry is shown. In section 3, an alternate extended Kronig-Penney model in the form of a ladder is analyzed. In section 4, the natural extension of the asymmetric quantum ladder to the two-dimensional rectangular lattice with alternating δ , δ' layers is considered. Section 5 details the method to realize both mathematical models with conventional δ coupling vertices. The last section, section 6, concludes with a summery.

2. Double-stranded chain with singular vertices

We start our investigation of periodic lattice structures containing non-conventional vertex couplings with the simplest case, i.e., the double-stranded Kronig-Penney model with quantum graph vertices (Fig. 1). We examine the energy eigenstates of a quantum particle residing on

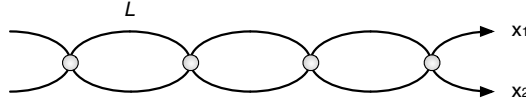


Figure 1: Rings of double-stranded Kronig-Penney lattice connected by nodes with singular interactions.

this structure. Due to the Bloch theorem, it is sufficient to consider a single unit segment of the lattice $x_1 \in [0, L)$ and $x_2 \in [0, L)$ as shown in Fig. 2. The wave function is given in the form

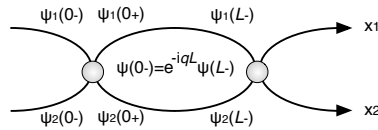


Figure 2: Elementary cell of the lattice and quasi-periodicity of wave function.

$$\begin{aligned} \psi_1(x_1) &= \alpha_1 e^{ikx_1} + \beta_1 e^{-ikx_1}, \\ \psi_2(x_2) &= \alpha_2 e^{ikx_2} + \beta_2 e^{-ikx_2} \end{aligned} \quad (1)$$

and from the quasi-periodicity condition we have

$$\begin{aligned}\psi_1(0_-) &= e^{-iqL}\psi_1(L_-), & \psi'_1(0_-) &= e^{-iqL}\psi'_1(L_-), \\ \psi_2(0_-) &= e^{-iqL}\psi_2(L_-), & \psi'_2(0_-) &= e^{-iqL}\psi'_2(L_-),\end{aligned}\quad (2)$$

which yield the relations

$$\begin{aligned}\psi_1(0_-) &= e^{-iqL}(e^{ikL}\alpha_1 + e^{-ikL}\beta_1), & \psi'_1(0_-) &= ike^{-iqL}(e^{ikL}\alpha_1 - e^{-ikL}\beta_1), \\ \psi_2(0_-) &= e^{-iqL}(e^{ikL}\alpha_2 + e^{-ikL}\beta_2), & \psi'_2(0_-) &= ike^{-iqL}(e^{ikL}\alpha_2 - e^{-ikL}\beta_2).\end{aligned}\quad (3)$$

The most general connection condition at the graph vertex $x = 0$ is given in terms of the vectors

$$\Psi = \begin{pmatrix} \psi_1(0_-) \\ \psi_1(0_+) \\ \psi_2(0_-) \\ \psi_2(0_+) \end{pmatrix}, \quad \Psi' = \begin{pmatrix} -\psi'_1(0_-) \\ \psi'_1(0_+) \\ -\psi'_2(0_-) \\ \psi'_2(0_+) \end{pmatrix}, \quad (4)$$

by

$$B\Psi' + A\Psi = 0, \quad (5)$$

where A and B are complex 4×4 matrices and satisfy the requirements

- $\text{rank}(A|B) = 4$,
 - the matrix AB^* is self-adjoint,
- (6)

where $(A|B)$ is a 4×8 matrix formed from columns of A and B . [10] The choice of matrices A and B is not unique as the equation (5) can be multiplied from the left by an arbitrary non-degenerate matrix. One convenient way of representing connection conditions (5) is transforming them into the ST -form [9], which is the block form

$$\begin{pmatrix} I^{(m)} & T \\ 0 & 0 \end{pmatrix} \Psi' = \begin{pmatrix} S & 0 \\ -T^* & I^{(4-m)} \end{pmatrix} \Psi, \quad (7)$$

where $m \in \{0, 1, 2, 3, 4\}$. Here, $I^{(m)}$ is the identity matrix $m \times m$, T is a complex matrix of size $m \times (4 - m)$ and S is a Hermitian matrix of order r . Since the wave functions at $x = 0_+$ are given in terms of coefficients α_j and β_j as

$$\begin{aligned}\psi_1(0_+) &= \alpha_1 + \beta_1, & \psi'_1(0_+) &= ik(\alpha_1 - \beta_1), \\ \psi_2(0_+) &= \alpha_2 + \beta_2, & \psi'_2(0_+) &= ik(\alpha_2 - \beta_2),\end{aligned}\quad (8)$$

the quasi-periodicity conditions of wave function (3) can be rewritten in terms of four-vector

$$V = \begin{pmatrix} \alpha_1 \\ \beta_1 \\ \alpha_2 \\ \beta_2 \end{pmatrix}, \quad (9)$$

as

$$\Psi = e^{-iqL}FV, \quad \Psi' = ike^{-iqL}GV, \quad (10)$$

where the 4×4 matrices F and G are defined by

$$F = \begin{pmatrix} e^{ikL} & e^{-ikL} & 0 & 0 \\ e^{iqL} & e^{iqL} & 0 & 0 \\ 0 & 0 & e^{ikL} & e^{-ikL} \\ 0 & 0 & e^{iqL} & e^{iqL} \end{pmatrix}, \quad G = \begin{pmatrix} -e^{ikL} & e^{-ikL} & 0 & 0 \\ e^{iqL} & -e^{iqL} & 0 & 0 \\ 0 & 0 & -e^{ikL} & e^{-ikL} \\ 0 & 0 & e^{iqL} & -e^{iqL} \end{pmatrix}. \quad (11)$$

In principle, a scaling parameter is required in the connection conditions (5) or (7) to compensate the differences in the length dimensions of Ψ and Ψ' [11]. But in practice, it could be dropped since it can be absorbed into the definition of the length unit. The equation specifying the connection condition $A\Psi + B\Psi' = 0$ now reads $(AF + ikBG)V = 0$, and a nontrivial solution can be obtained only with the condition

$$\det [AF + ikBG] = 0. \quad (12)$$

Since the whole family of all possible vertex couplings is too large to handle, we limit our choice to a subfamily of $m = 2$ in the form

$$T = \begin{pmatrix} a & b \\ a & b \end{pmatrix}, \quad S = \begin{pmatrix} c & cd \\ cd & cd^2 \end{pmatrix}. \quad (13)$$

For such boundary conditions we obtain an explicit solution in the form

$$\cos qL = \frac{R \pm \sqrt{R^2 + 2abkS}}{4abk}, \quad (14)$$

where

$$\begin{aligned} R &= (a - b)^2 k \cos kL + c[(a^2 + b^2)(d - 1)^2 + d^2 + 1] \sin kL, \\ S &= (2a^2 + 2b^2 - 1)k + (2a^2 + 2b^2 + 1)k \cos 2kL - c[(a^2 + b^2)(d - 1)^2 + d^2 + 1] \sin 2kL. \end{aligned} \quad (15)$$

Note that there are two sets of bands, which may overlap, each corresponding to plus and minus of the composite signs. For each band, we calculate the quantum flux of the particle going through the top and bottom strands, which are obtained from the formula $J_j = \frac{\hbar}{2mi} (\psi_j^* \psi'_j - \psi_j \psi_j'^*)$ ($j = 1, 2$) with wave functions (1). We have

$$\begin{aligned} J_1 &= \frac{k\hbar}{m} (|\alpha_1|^2 - |\beta_1|^2), \\ J_2 &= \frac{k\hbar}{m} (|\alpha_2|^2 - |\beta_2|^2). \end{aligned} \quad (16)$$

Notice that from the Bloch theorem, it follows that the currents (16) are conserved along the chain. As we did not fix the boundary conditions of the whole lattice, the wave function is not normalizable and the absolute values of J_i carry no physical meaning. The ratio between them is physical, on the other hand, and it is the exact quantity of our primary interest: Its absolute value is the measure of the asymmetry of current flows between two strands, and its sign determines their relative directions.

In Fig. 3 and Fig. 4 there are shown four sets of numerical examples obtained with combinations $b = \pm a$ and $d = \pm 1$. The values of other parameters are set to be $a = \frac{1}{3}$ and $c = 8$. For

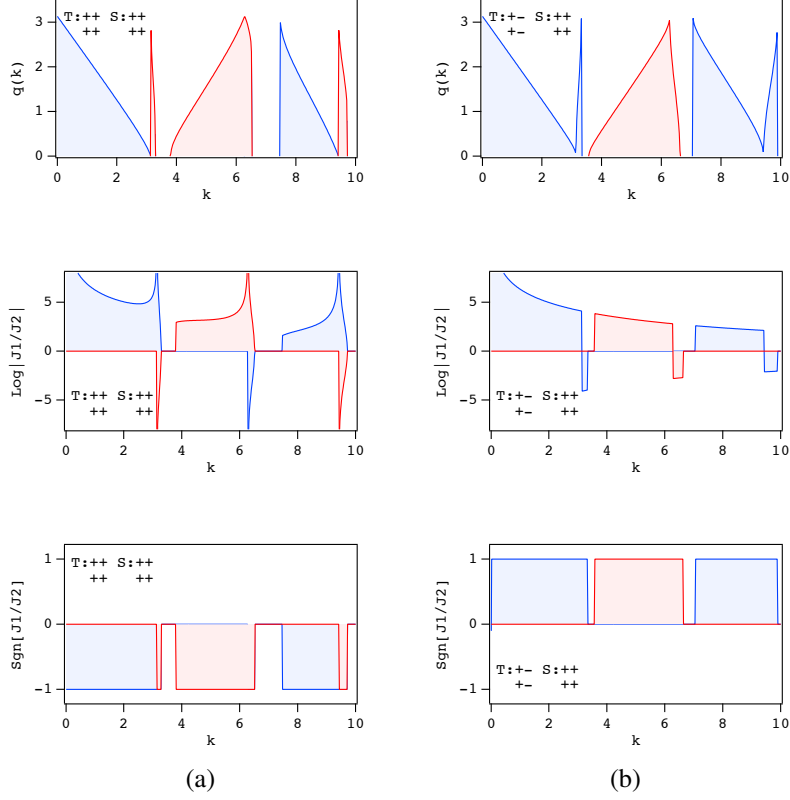


Figure 3: The band structure (top), the logarithm of the absolute value of flux ratio (middle), and the relative flux direction (bottom) are plotted as the function of the particle energy for the coupling parameter (a) $a = b = \frac{1}{3}$, $c = 8$, $d = 1$, and (b) $a = \frac{1}{3}$, $b = -\frac{1}{3}$, $c = 8$, $d = 1$. The red and blue lines correspond to the two solutions of secular equation (14), and the shaded areas indicate energy bands of the spectrum. The plus and minus signs in the inlet caption refer to the structure of matrices T and S in (13).

each set of parameters, we display the energy bands, the logarithm of $|J_1/J_2|$, and the relative sign $\text{sgn}[J_1/J_2]$, each as functions of particle energy.

The asymmetric quantum transport, with respect to the two strands, is evident. In each of the alternating regions within a band, the transport is supported mainly in one of the two strands. With different choices of system parameters, various patterns of asymmetry variations are observed as we move from one energy band to the next one.

Particularly intriguing examples of alternating flux asymmetry are found in the case $b = -a$, depicted in Figs. 3 (b) and 4 (b); With the choice $d > 0$, we find that the localization of flux strength changes from one strand to another in successive bands, while the relative direction stays positive all the way, as seen from Fig. 3 (b). In the case $d < 0$, we observe that the relative flux direction change in successive bands, while the relative strength remains one-sided, as can be noticed from Fig. 4 (b).

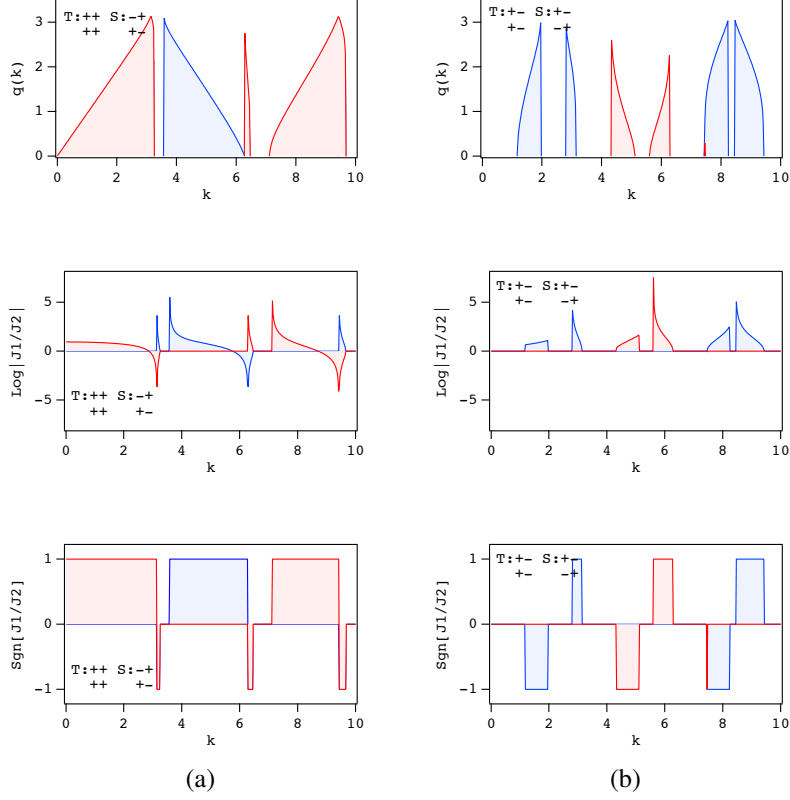


Figure 4: The band structure (top), the logarithm of the flux ratio (middle), and the relative flux direction (bottom) are plotted as the function of the particle energy for the coupling parameter (a) $a = b = \frac{1}{3}$, $c = 8$, $d = -1$, and (b) $a = \frac{1}{3}$, $b = -\frac{1}{3}$, $c = 8$, $d = -1$. The red and blue lines correspond to the two solutions of secular equation (14), and the shaded areas indicate energy bands of the spectrum. the plus and minus signs in the inlet caption refer to the structure of matrices T and S in (13).

3. Asymmetric Kronig-Penny ladder

In this section we will give a realization of a double-stranded Kronig-Penny system by asymmetric periodic ladder with internal lines. We will obtain the chained ring model of the previous section as a zero-size limit case of internal lines.

Consider a ladder-like quantum graph made up of two parallel lines linked at regular intervals by internal lines on both parallel lines (Fig. 5). Applying the Bloch theorem again, we examine a single unit segment of the lattice, which is described by coordinates $x_1 \in [0, L]$, $x_2 \in [0, L]$ and $x_\ell \in [0, \ell]$. The wave function is given in the form

$$\begin{aligned}
 \psi_1(x_1) &= \alpha_1 e^{ikx_1} + \beta_1 e^{-ikx_1}, \\
 \psi_2(x_2) &= \alpha_2 e^{ikx_2} + \beta_2 e^{-ikx_2}, \\
 \phi(x_\ell) &= \alpha_\ell e^{ikx_\ell} + \beta_\ell e^{-ikx_\ell}.
 \end{aligned} \tag{17}$$

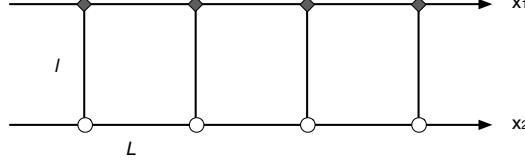


Figure 5: Asymmetric quantum ladder with different kind of vertex couplings at black and white vertices

In the unit segment there are two junctions, $(x_1 = 0 \ \& \ x_\ell = 0)$ and $(x_2 = 0 \ \& \ x_\ell = \ell)$. At each junction we consider the vectors Ψ_t, Ψ'_t and Ψ_b, Ψ'_b , which are respectively defined by

$$\Psi_t = \begin{pmatrix} \psi_1(0_-) \\ \psi_1(0_+) \\ \phi(0) \end{pmatrix}, \Psi'_t = \begin{pmatrix} -\psi'_1(0_-) \\ \psi'_1(0_+) \\ \phi'(0) \end{pmatrix}, \quad (18)$$

and

$$\Psi_b = \begin{pmatrix} \psi_2(0_-) \\ \psi_2(0_+) \\ \phi(\ell) \end{pmatrix}, \Psi'_b = \begin{pmatrix} -\psi'_2(0_-) \\ \psi'_2(0_+) \\ -\phi'(\ell) \end{pmatrix}. \quad (19)$$

The properties of the junctions are determined by the linear matrix equations of Ψ and Ψ' . We consider different types of vertex interactions at top and bottom nodes of the ladder,

$$\begin{pmatrix} 1 & 0 & a_1 \\ 0 & 1 & a_2 \\ 0 & 0 & 0 \end{pmatrix} \Psi'_t - \begin{pmatrix} v_{11} & v_{12} & 0 \\ v_{21} & v_{22} & 0 \\ -a_1^* & -a_2^* & 1 \end{pmatrix} \Psi_t = 0, \\ \begin{pmatrix} 1 & b_1 & b_2 \\ 0 & 0 & 0 \\ 0 & 0 & 0 \end{pmatrix} \Psi'_b - \begin{pmatrix} u & 0 & 0 \\ -b_1^* & 1 & 0 \\ -b_2^* & 0 & 1 \end{pmatrix} \Psi_b = 0, \quad (20)$$

where we used notations (18) (19) and had conditions $v_{11} = v_{11}^*, v_{22} = v_{22}^*, v_{12} = v_{21}^*, u = u^*$.

Let us consider the limit case $\ell \ll \frac{1}{k}$, where we have

$$\begin{aligned} \phi(\ell) &= \alpha_\ell e^{ik\ell} + \beta_\ell e^{-ik\ell} \approx \alpha_\ell + \beta_\ell = \phi(0), \\ \phi'(\ell) &= ik\alpha_\ell e^{ik\ell} - ik\beta_\ell e^{-ik\ell} \approx ik\alpha_\ell - ik\beta_\ell = \phi'(0). \end{aligned} \quad (21)$$

Expelling the function ϕ , we rewrite matrix equations (20) in the form

$$\begin{pmatrix} 1/a_1 & -1/a_2 & 0 & 0 \\ 1/a_1 & 0 & 1/b_2 & b_1/b_2 \\ 0 & 0 & 0 & 0 \\ 0 & 0 & 0 & 0 \end{pmatrix} \begin{pmatrix} \psi'_1 \\ \psi'_2 \\ \psi'_3 \\ \psi'_4 \end{pmatrix} - \begin{pmatrix} \frac{v_{11}}{a_1} - \frac{v_{21}}{a_2} & \frac{v_{12}}{a_1} - \frac{v_{22}}{a_2} & 0 & 0 \\ \frac{v_{11}}{a_1} & \frac{v_{12}}{a_1} & \frac{u}{b_2} & 0 \\ 0 & 0 & -b_1^* & 1 \\ -a_1^* & -a_2^* & b_2^* & 0 \end{pmatrix} \begin{pmatrix} \psi_1 \\ \psi_2 \\ \psi_3 \\ \psi_4 \end{pmatrix} = 0. \quad (22)$$

Applying transformations introduced in paper [9], the boundary conditions (22) can be rewritten in the *ST-form*

$$\begin{pmatrix} 1 & 0 & a_1/b_2 & b_1 a_1/b_2 \\ 0 & 1 & a_2/b_2 & b_1 a_2/b_2 \\ 0 & 0 & 0 & 0 \\ 0 & 0 & 0 & 0 \end{pmatrix} \begin{pmatrix} \psi'_1 \\ \psi'_2 \\ \psi'_3 \\ \psi'_4 \end{pmatrix} - \begin{pmatrix} v_{11} + \frac{ua_1 a_1^*}{b_2 b_2^*} & v_{12} + \frac{ua_1 a_2^*}{b_2 b_2^*} & 0 & 0 \\ v_{21} + \frac{ua_1^* a_2}{b_2 b_2^*} & v_{22} + \frac{ua_2^* a_2}{b_2 b_2^*} & 0 & 0 \\ -a_1^*/b_2^* & -a_2^*/b_2^* & 1 & 0 \\ -b_1^* a_1^*/b_2^* & -b_1^* a_1^*/b_2^* & 0 & 1 \end{pmatrix} \begin{pmatrix} \psi_1 \\ \psi_2 \\ \psi_3 \\ \psi_4 \end{pmatrix} = 0. \quad (23)$$

Considering the special case $u = 0$, $a_2 = a_1$, $b_1 = \pm 1$, $b_2 = 1$ and $v_{11} = v_{22} = \pm v_{12}$ we obtain the boundary conditions investigated in previous section. Particularly, we can derive effective connection conditions with matrix coefficients (7), (13), if we insert vertex couplings at black and white nodes in the following way:

$$\begin{pmatrix} 1 & 0 & a \\ 0 & 1 & a \\ 0 & 0 & 0 \end{pmatrix} \Psi'_t - \begin{pmatrix} c & cd & 0 \\ cd & cd^2 & 0 \\ -a & -a & 1 \end{pmatrix} \Psi_t = 0,$$

$$\begin{pmatrix} 1 & b/a & 1 \\ 0 & 0 & 0 \\ 0 & 0 & 0 \end{pmatrix} \Psi'_b - \begin{pmatrix} 0 & 0 & 0 \\ -b/a & 1 & 0 \\ -1 & 0 & 1 \end{pmatrix} \Psi_b = 0. \quad (24)$$

In general case, depending on the values of the parameters in connection conditions at graph vertices, it can be revealed a large variety of the spectrum of bound state and complicated flux behaviour through ladder lanes. Therefore, let us focus on an asymmetric ladder with more simplified boundary conditions at its vertices. Particularly, we require δ potential-type connection conditions for the upper junctions:

$$\begin{pmatrix} 1 & 1 & 1 \\ 0 & 0 & 0 \\ 0 & 0 & 0 \end{pmatrix} \Psi'_t - \begin{pmatrix} v & 0 & 0 \\ -1 & 1 & 0 \\ -1 & 0 & 1 \end{pmatrix} \Psi_t = 0. \quad (25)$$

For the bottom junctions, we assume that the connection conditions are more “exotic”, in order to see whether that produces any interesting phenomena. Specifically, we impose the symmetrized δ' -type condition

$$\begin{pmatrix} 1 & 0 & -1 \\ 0 & 1 & -1 \\ 0 & 0 & u \end{pmatrix} \Psi'_b - \begin{pmatrix} 0 & 0 & 0 \\ 0 & 0 & 0 \\ 1 & 1 & 1 \end{pmatrix} \Psi_b = 0. \quad (26)$$

Now the problem became finding the solution (1) which would satisfy the connection conditions (25),(31) and quasi-periodicity of wave functions ψ_1 and ψ_2 (Fig 6). Substituting the limits of wave function (3) into the boundary conditions and completing a straightforward calculation, we derive a relation between the energy $E = k^2$ and quasimomentum q

$$2 \cos(2Lq) - 2 \cos(Lq) \sin(kL) \left(ku + \frac{v}{k} \right) + \sin(2kL) \left(ku - \frac{v}{k} \right) - \sin^2(kL)(uv + 5) - 2 + \tan(k\ell) \left(\sin^2(kL) \left(\frac{v}{k} - ku \right) + 2 \sin(2kL) \right) = 0. \quad (27)$$

From the secular equation (27), one can easily find the Bloch wave number q by solving the quadratic equation. For the given energy, we have either no real solution, one solution, or two

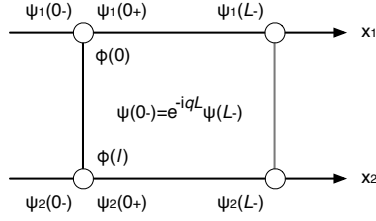


Figure 6: Unit chain of the ladder lattice and the condition of quasi-periodicity of the wave function.

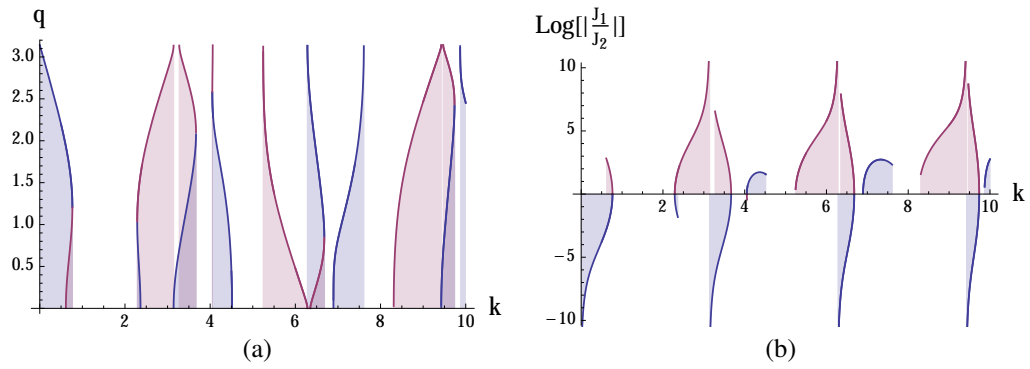


Figure 7: Numerical plot of two solutions of secular equation shown by shaded red and blue lines (a) and the corresponding pattern of flux asymmetry (b) for the following values of parameters: $u = 1, v = 1, L = 1, \ell = 1$.

solutions. Two solutions of secular equation are depicted in Fig. 7(a) by blue and red lines which have overlapping areas. Thus, we derived a band structure of spectrum containing gaps and zones with single or double solutions.

We calculate the quantum currents through upper and lower strands, J_1 and J_2 with (16) just like in the previous section. It turns out that the currents are always opposite to each other. The dependence of the logarithm of the absolute value of the ratio J_1 and J_2 on wave number k is shown in Fig. 7(b), which shows the flux asymmetry between two strands. Thus, we conclude that the introduction of different types of couplings at vertices of lattice strands leads to alternating asymmetry of currents, as we move from one band to another. Such flux behaviour indicates the importance of the role of boundary conditions at lattice vertices and reminds one of the case of the chained ring model in the previous section.

4. 2D plane with δ and δ' layers

In this section we will consider a Kronig-Penney model on a 2D rectangular lattice with lattice constants L and ℓ . We will assume an alternating layer structure with δ and δ' vertices. Here also, due to the Bloch theorem, it is sufficient to examine the wave function in the unit segment and use boundary conditions at δ and δ' connections. Note that the lattice periods along x and y directions are L and 2ℓ respectively

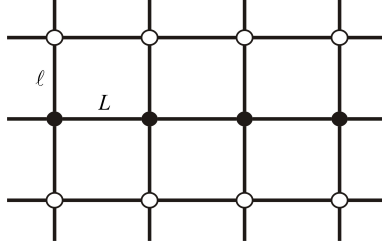


Figure 8: 2D extension of asymmetric quantum ladder with δ and δ' nodes.

$$\begin{aligned}
\psi_1(x_1) &= \alpha_1 e^{ikx_1} + \beta_1 e^{-ikx_1}, & 0 < x_1 < L, \\
\psi_2(x_2) &= \alpha_2 e^{ikx_2} + \beta_2 e^{-ikx_2}, & 0 < x_2 < L, \\
\phi(y) &= \alpha_3 e^{iky} + \beta_3 e^{-iky}, & 0 < y < \ell, \\
\phi(y) &= \alpha_4 e^{iky} + \beta_4 e^{-iky}, & \ell < y < 2\ell.
\end{aligned} \tag{28}$$

As in previous sections, we use notations Ψ_t , Ψ'_t , Ψ_b , and Ψ'_b defined by

$$\Psi_t = \begin{pmatrix} \psi_1(0_-) \\ \phi(0_-) \\ \psi_1(0_+) \\ \phi(0_+) \end{pmatrix}, \Psi'_t = \begin{pmatrix} -\psi'_1(0_-) \\ -\phi'(0_-) \\ \psi'_1(0_+) \\ \phi'(0_+) \end{pmatrix}, \Psi_b = \begin{pmatrix} \psi_2(0_-) \\ \phi(\ell_-) \\ \psi_2(0_+) \\ \phi(\ell_+) \end{pmatrix}, \Psi'_b = \begin{pmatrix} -\psi'_2(0_-) \\ -\phi'(\ell_-) \\ \psi'_2(0_+) \\ \phi'(\ell_+) \end{pmatrix} \tag{29}$$

and write the boundary conditions for δ junction in the form

$$\begin{pmatrix} 1 & 1 & 1 & 1 \\ 0 & 0 & 0 & 0 \\ 0 & 0 & 0 & 0 \\ 0 & 0 & 0 & 0 \end{pmatrix} \Psi'_t - \begin{pmatrix} v & 0 & 0 & 0 \\ -1 & 1 & 0 & 0 \\ -1 & 0 & 1 & 0 \\ -1 & 0 & 0 & 1 \end{pmatrix} \Psi_t = 0 \tag{30}$$

and for the symmetrized δ' -coupling

$$\begin{pmatrix} 1 & 0 & 0 & -1 \\ 0 & 1 & 0 & -1 \\ 0 & 0 & 1 & -1 \\ 0 & 0 & 0 & u \end{pmatrix} \Psi'_b - \begin{pmatrix} 0 & 0 & 0 & 0 \\ 0 & 0 & 0 & 0 \\ 0 & 0 & 0 & 0 \\ 1 & 1 & 1 & 1 \end{pmatrix} \Psi_b = 0. \tag{31}$$

The condition of quasiperiodicity of wave function along x and y directions gives

$$\begin{aligned}
\psi_1(0_-) &= e^{-iq_x L} (e^{ikL} \alpha_1 + e^{-ikL} \beta_1), & \psi'_1(0_-) &= ike^{-iq_x L} (e^{ikL} \alpha_1 - e^{-ikL} \beta_1), \\
\psi_2(0_-) &= e^{-iq_x L} (e^{ikL} \alpha_2 + e^{-ikL} \beta_2), & \psi'_2(0_-) &= ike^{-iq_x L} (e^{ikL} \alpha_2 - e^{-ikL} \beta_2), \\
\phi(0_-) &= e^{-2iq_y \ell} (e^{2ik\ell} \alpha_4 + e^{-2ik\ell} \beta_4), & \phi'(0_-) &= ike^{-2iq_y \ell} (e^{2ik\ell} \alpha_4 - e^{-2ik\ell} \beta_4),
\end{aligned} \tag{32}$$

To obtain the spectral equation, more tedious calculations are needed, compared to that of the ladder case. However, the procedure is quite similar to previous case and the secular equation

reads

$$\begin{aligned} \cos(2\ell q_y) = & \frac{1}{16 \sin^2(kL)} \left(\sin(kL) \left(8ku + \frac{8v}{k} \right) (\cos(2k\ell) + 1) \cos(Lq_x) \right. \\ & - 8(\cos(2k\ell) + 1) \sin(2Lq_x) + \left(\frac{4v}{k} - 4ku \right) (\sin(2kL) - \sin(2k\ell) + \sin(2k(L + \ell))) \\ & \left. + uv \cos(2k(L - \ell)) - 2uv + (uv + 16) \cos(2k(L + \ell)) + (2uv + 8) (\cos(2kL) - \cos(2k\ell)) \right). \end{aligned} \quad (33)$$

The expression (33) can be simplified if we assume $\ell = L$, which reduces it into

$$\begin{aligned} \cos(2Lq_y) = & \frac{1}{4 \sin^2(kL)} \left((\sin(kL) + \sin(3kL)) \left(ku + \frac{v}{k} \right) \cos(Lq_x) \right. \\ & \left. - 2(\cos(2kL) + 1) \cos(2Lq_x) + \sin(4kL) \left(\frac{v}{k} - ku \right) + \left(\frac{uv}{4} + 4 \right) \cos(4kL) - \frac{uv}{4} \right). \end{aligned} \quad (34)$$

Thus, we obtained a spectral equation, which gives a connection among Bloch wave numbers q_x and q_y , and the energy $E = k^2$. To define the state of the system, we need to fix not only energy, but also one of the Bloch numbers; using the spectral equation (33), we can obtain the second Bloch number. Numerical calculations show that energy gaps appear in the spectrum, i.e. there is some range of values for k for which the equation (34) has no real solution for q_x and q_y . All gaps have period $2\pi L$ and in the particular case $u = 1, v = 1, L = 1$ we have $4.431 \lesssim k \lesssim 4.712$ for the first gap.

To compare particle flux on x and y directions, we have to take into account four types of currents

$$\begin{aligned} J_1^x &= \frac{k\hbar}{m} (|\alpha_1|^2 - |\beta_1|^2), \\ J_2^x &= \frac{k\hbar}{m} (|\alpha_2|^2 - |\beta_2|^2), \\ J_1^y &= \frac{k\hbar}{m} (|\alpha_3|^2 - |\beta_3|^2), \\ J_2^y &= \frac{k\hbar}{m} (|\alpha_4|^2 - |\beta_4|^2). \end{aligned} \quad (35)$$

In the case of our model for the certain values of energies and Bloch wave numbers, we have no currents on either x or y directions. For example, assuming again $u = 1, v = 1, \ell = L = 1$ we found out $J_1^x = J_2^x = J_1^y = J_2^y = 0$ for $q_x = 1, k = \pi/2$. There are also special values of energy and Bloch wave q_x , for which the particle current disappears only along the vertical or horizontal lattice bonds. For instance, $J_1^x = J_2^x = 0, J_1^y \neq 0, J_2^y \neq 0$ when $q_x = \pi p$ ($p = 0, \pm 1, \pm 2, \dots$) and $J_1^y = J_2^y = J_1^x = 0, J_2^x \neq 0$ if $q_x = 1, k \approx 0.753$ (the case $J_2^x = 0, J_1^x \neq 0$ corresponds to $q_x = -1$).

5. Realization of quantum graphs with δ vertices

In this section we give a construction scheme for the physical realization of non-conventional vertex couplings of a double-stranded lattice. We will use an approximation method of arbitrary

singular vertices by quantum graphs carrying only δ -couplings and constant vector potentials, [9] which is a generalisation of the ‘‘singular local potential realisation’’ of the δ' coupling on a line [12, 13]. Referring the reader to the original papers for full details, let us very briefly review the basic points of the scheme:

- Separate n edges of the star graph and connect nodes i and j by lines of the length $2d_0$ if one of the following three conditions is satisfied

- (1) $j \leq m, k \geq m + 1$, and $T_{jk} \neq 0$ (or $j \geq m + 1, k \leq m$, and $T_{kj} \neq 0$),
- (2) $j \leq m, k \leq m$ and $(\exists l \geq m + 1)(T_{jl} \neq 0 \wedge T_{kl} \neq 0)$,
- (3) $j \leq m, k \leq m, S_{jk} \neq 0$, and the previous condition is not satisfied,

where the rows of the matrix T are indexed from 1 to m and the columns from $m + 1$ to n .

- Apply a δ -coupling with interaction parameter v_j at the j -th node for all $1 \leq j \leq n$ and add a δ -potential with parameter w_{jk} at the centre of the constructed line (j, k) for all $1 \leq k \leq N_j$, where N_j is a number of vertices joined to the j -th one. Place also constant vector potentials $A_{(j,l)}$ and $A_{(l,k)} = -A_{(j,l)}$ on the segments (j, l) and (l, k) respectively, where l is the centre of the line (j, k) $1 \leq l \leq N_j$.
- The values of δ -interaction parameters v_j, w_{jk} and vector potentials $A_{(j,k)}$ depend on size parameter d_0 and are determined by the following way:

- (1) If $j \leq m$ and $k \geq m + 1$ then

$$\begin{aligned} A_{(j,k)}(d_0) &= \begin{cases} \frac{1}{2d_0} \arg T_{jk} & \text{if } \operatorname{Re} T_{jk} \geq 0, \\ \frac{1}{2d_0} (\arg T_{jk} - \pi) & \text{if } \operatorname{Re} T_{jk} < 0, \end{cases} \\ v_k(d_0) &= \frac{1 - N_k + \sum_{h=1}^m \langle T_{hk} \rangle}{d_0}, \\ w_{jk}(d_0) &= \frac{1}{d_0} \left(-2 + \frac{1}{\langle T_{jk} \rangle} \right), \end{aligned} \quad (36)$$

where the symbol $\langle \cdot \rangle$ means

$$\langle c \rangle = \begin{cases} |c| & \text{if } \operatorname{Re} c \geq 0, \\ -|c| & \text{if } \operatorname{Re} c < 0. \end{cases}$$

- (2) In the case $j \leq m, k \leq m$ we have

$$\begin{aligned} A_{(j,k)}(d_0) &= \begin{cases} \frac{1}{2d_0} \arg \left(d_0 S_{jk} + \sum_{l=m+1}^n T_{jl} \overline{T_{kl}} \right) & \text{if } \operatorname{Re} \left(d_0 \cdot S_{jk} + \sum_{l=m+1}^n T_{jl} \overline{T_{kl}} \right) \geq 0, \\ \frac{1}{2d_0} \left[\arg \left(d_0 S_{jk} + \sum_{l=m+1}^n T_{jl} \overline{T_{kl}} \right) - \pi \right] & \text{if } \operatorname{Re} \left(d_0 S_{jk} + \sum_{l=m+1}^n T_{jl} \overline{T_{kl}} \right) < 0, \end{cases} \\ v_j(d_0) &= S_{jj} - \frac{N_j}{d_0} - \sum_{k=1}^m \left\langle S_{jk} + \frac{1}{d_0} \sum_{l=m+1}^n T_{jl} \overline{T_{kl}} \right\rangle + \frac{1}{d_0} \sum_{l=m+1}^n (1 + \langle T_{jl} \rangle) \langle T_{jl} \rangle, \\ w_{jk}(d_0) &= -\frac{1}{d_0} \left(2 + \left\langle d_0 \cdot S_{jk} + \sum_{l=m+1}^n T_{jl} \overline{T_{kl}} \right\rangle^{-1} \right). \end{aligned} \quad (37)$$

It can be shown that the constructed graph converges to desired singular vertex coupling in the norm-resolvent sense [9]. Also note that this approximation scheme and choice of parameters are not unique.

We represent singular vertices of double-stranded quantum graph in two alternative ways. For the sake of simplicity, let us consider only the case $b = a$ and $d = 1$ in the matrices (13). At first, we directly apply the construction scheme (36), (37) to design a quantum star graph with connection conditions

$$\begin{pmatrix} c & c & 0 & 0 \\ c & c & 0 & 0 \\ -a & -a & 1 & 0 \\ -a & -a & 0 & 1 \end{pmatrix} \Psi - \begin{pmatrix} 1 & 0 & a & a \\ 0 & 1 & a & a \\ 0 & 0 & 0 & 0 \\ 0 & 0 & 0 & 0 \end{pmatrix} \Psi' = 0 \quad (38)$$

Then we give the second approximating way of the same vertices by implementing the asymmetric ladder system (see Section 3) with boundary conditions at the vertices

$$\begin{pmatrix} 1 & 0 & a \\ 0 & 1 & a \\ 0 & 0 & 0 \end{pmatrix} \Psi'_t - \begin{pmatrix} c & c & 0 \\ c & c & 0 \\ -a & -a & 1 \end{pmatrix} \Psi_t = 0, \\ \begin{pmatrix} 1 & 1 & 1 \\ 0 & 0 & 0 \\ 0 & 0 & 0 \end{pmatrix} \Psi'_b - \begin{pmatrix} 0 & 0 & 0 \\ -1 & 1 & 0 \\ -1 & 0 & 1 \end{pmatrix} \Psi_b = 0. \quad (39)$$

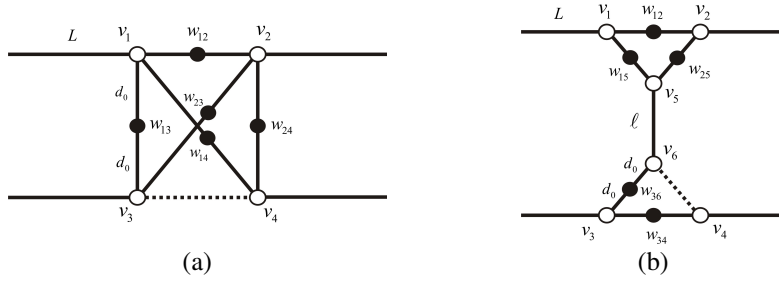


Figure 9: Two alternative ways of approximating a double-stranded junction by delta vertices.

Let us split the graph nodes of the double-stranded chain and quantum ladder, as shown in figures 9a and 9b, and connect the free endpoints by wires. Note that the edges shown by a dashed lines are not connected according to our construction scheme. As all the parameters in boundary conditions (38) and (39) are real, we will not need to apply vector potentials to the connecting lines. The values of δ -potential strengths at nodes and in the centres of graph edges, are determined by

$$v_1 = v_2 = -c - \frac{1}{d_0}(2a^2 - 2a + 3), \quad v_3 = v_4 = \frac{1}{d_0}(-1 + 2a), \\ w_{12} = -\frac{1}{d_0}\left(2 + \frac{1}{d_0c + 2a^2}\right), \quad w_{13} = w_{14} = w_{23} = w_{24} = \frac{1}{d_0}\left(-2 + \frac{1}{a}\right) \quad (40)$$

for the figure 9a and

$$v_1 = v_2 = -c - \frac{1}{d_0}(a^2 - a + 2), \quad v_3 = 0, \quad v_4 = v_6 = \frac{1}{d_0}, \quad v_5 = \frac{1}{d_0}(-1 + 2a),$$

$$w_{12} = -\frac{1}{d_0}\left(2 + \frac{1}{d_0 c + a^2}\right), \quad w_{15} = w_{25} = \frac{1}{d_0}\left(-2 + \frac{1}{c}\right), \quad w_{34} = w_{36} = -\frac{1}{d_0} \quad (41)$$

for the figure 9b. Thus, the boundary conditions (38) can be achieved in the shrinking limit $d_0 \ll \frac{1}{k}$ for the double-stranded chain and $d_0 \ll \ell \ll \frac{1}{k}$ for the ladder lattice.

6. Summary and prospects

In this paper, we have considered minimal double-stranded extensions of the celebrated Kronig-Penney model and uncovered unexpected exotic features in the pattern of fluxes that go through the two strands. The key to the discovery has been the employment of non-conventional vertex couplings, which, at the first glance, seems rather artificial. We have shown, however, that the model can be regarded as a mathematical abstraction of a more realistic periodic two-lane ladder with conventional δ -couplings, albeit with more complicated internal graph structures.

The investigation of straightforward extensions to the chains with triple and more strands can be accomplished by direct computations. The more challenging problem is the full analysis of a layered two-dimensional Kronig-Penney lattice. The identification of parameter ranges which permit a symmetric flux in two dimensional models should be considered of great importance for designing and developing quantum devices.

Acknowledgments

The authors thank Michelle Noyes for technical assistance in the preparation of this paper. This research was supported by the Japan Ministry of Education, Culture, Sports, Science and Technology under the Grant number 24540412.

References

- [1] Y. Avishai and J.M. Luck: Quantum percolation and ballistic conductance on a lattice of wires, *Phys. Rev. B* **45** (1992) 1074.
- [2] J. Gratus, C. J. Lambert, S.J. Robinson, and R. W. Tucker: Quantum mechanics on graphs, *J. Phys. A* **27** (1994) 6881.
- [3] P. Kuchment: Graph models of wave propagation in thin structures, *Waves in Random Media* **12** (2002) R1.
- [4] T. Cheon and T. Shigehara: Continuous Spectra of Generalized Kronig-Penney Model, *J. Phys. Soc. Jpn.* **73** (2006) 2986.
- [5] P. Exner: Lattice Kronig-Penney model, *Phys. Rev. Lett.* **74** (1995) 3503.
- [6] H. Niikuni: Spectra of Periodic Schrödinger Operators on the Degenerate Zigzag Nanotube with δ Type Vertex Conditions, *Integr. Equ. Oper. Theory* **79** (2014) 477.
- [7] P. Exner and S.S. Manko: Spectra of magnetic chain graphs: coupling constant perturbations, arXiv:1412.6089.
- [8] R. de L. Kronig and W. G. Penney: Quantum Mechanics of Electrons in Crystal Lattices, *Proc. Roy. Soc. (London)* **A 130** (1931) 499.
- [9] T. Cheon, P. Exner and O. Turek: Approximation of a general singular vertex coupling in quantum graphs, *Ann. of Phys. A* **325** (2011) 548.
- [10] V. Kostrykin, R. Schrader: Kirchhoff's rule for quantum wires, *J. Phys. A: Math. Gen.* **32** (1999) 595.
- [11] T. Fülöp and I. Tsutsui: A free particle on a circle with point interaction, *Phys. Lett.* **A264** (2000) 366.
- [12] T. Cheon and T. Shigehara: Realizing discontinuous wave functions with renormalized short-range potentials, *Phys. Lett. A* **243** (1998) 111.
- [13] P. Exner, H. Neidhardt and V.A. Zagrebnov: Potential approximations to δ' : an inverse Klauder phenomenon with norm-resolvent convergence, *Commun. Math. Phys.* **224** (2001) 593.